# POZ-, AT-hook-, and Zinc Finger-containing Protein (PATZ) Interacts with Human Oncogene B Cell Lymphoma 6 (BCL6) and Is Required for Its Negative Autoregulation*

Raffaela Pero[‡], Dario Palmieri[‡§], Tiziana Angrisano[‡], Teresa Valentino[‡], Antonella Federico[‡], Renato Franco[¶], Francesca Lembo[‖], Andres J. Klein-Szanto[**], Luigi Del Vecchio[‡‡§§], Donatella Montanaro[§§], Simona Keller[‡§§], Claudio Arra[¶], Vasiliki Papadopoulou[¶¶], Simon D. Wagner[¶¶], Carlo M. Croce[§], Alfredo Fusco[‡], Lorenzo Chiariotti[‡‖1], and Monica Fedele[‡2]

From the [‡]Dipartimento di Biologia e Patologia Cellulare e Molecolare and the Istituto di Endocrinologia ed Oncologia Sperimentale, Università di Napoli "Federico II" and Consiglio Nazionale delle Ricerche (CNR), 80131 Naples, Italy, the [§]Department of Molecular Virology, Immunology and Medical Genetics, Comprehensive Cancer Center, Ohio State University, Columbus, Ohio 43210, the [¶]Istituto Nazionale dei Tumori, Fondazione Pascale, 80131 Naples, Italy, the [‖]Dipartimento di Chimica Farmaceutica e Tossicologica, Università di Napoli "Federico II", 80131 Naples, Italy, the [**]Department of Pathology, Fox-Chase Cancer Center, Philadelphia, Pennsylvania 19111, the [‡‡]Dipartimento di Biochimica e Biotecnologie Mediche, Università di Napoli "Federico II", 80131 Naples, Italy, the [§§]CEINGE, Biotecnologie Avanzate, 80145 Naples, Italy, and the [¶¶]Department of Cancer Studies and Molecular Medicine, University of Leicester, Leicester LE1 7RH, United Kingdom

**Background:** PATZ is a transcription factor, whose role in cancer is still under debate.
**Results:** PATZ interacts with BCL6 and negatively modulates its expression. Consistently, *Patz1* knockdown mice showed up-regulation of BCL6 expression and BCL6-dependent B cell neoplasias.
**Conclusion:** PATZ is a tumor suppressor that acts by cooperating with BCL6 in its negative autoregulation.
**Significance:** This work helps in understanding the pathology of BCL6-expressing lymphomas in which *BCL6* is not mutated.

The *PATZ1* gene encoding a POZ/AT-hook/Kruppel zinc finger (PATZ) transcription factor, is considered a cancer-related gene because of its loss or misexpression in human neoplasias. As for other POZ/domain and Kruppel zinc finger (POK) family members, the transcriptional activity of PATZ is due to the POZ-mediated oligomer formation, suggesting that it might be not a typical transactivator but an architectural transcription factor, thus functioning either as activator or as repressor depending on the presence of proteins able to interact with it. Therefore, to better elucidate PATZ function, we searched for its molecular partners. By yeast two-hybrid screenings, we found a specific interaction between PATZ and BCL6, a human oncogene that plays a key role in germinal center (GC) derived neoplasias. We demonstrate that PATZ and BCL6 interact in germinal center-derived B lymphoma cells, through the POZ domain of PATZ. Moreover, we show that PATZ is able to bind the BCL6 regulatory region, where BCL6 itself acts as a negative regulator, and to contribute to negatively modulate its activity. Consistently, disruption of one or both *Patz1* alleles in mice causes focal expansion of thymus B cells, in which BCL6 is up-regulated. This phenotype was almost completely rescued by crossing Patz1^{+/−} with Bcl6^{+/−} mice, indicating a key role for Bcl6 expression in its development. Finally, a significant num-

ber of *Patz1* knock-out mice (both heterozygous and homozygous) also develop BCL6-expressing lymphomas. Therefore, the disruption of one or both *Patz1* alleles may favor lymphomagenesis by activating the BCL6 pathway.

The *PATZ1* gene encodes four main alternative proteins ranging from 537 to 687 amino acids that contain an N-terminal POZ domain, one or two AT-hooks in the central region, and four to six C2H2 zinc finger motifs at the C terminus (1–3). Both the AT-hooks and the POZ domain are characteristic of protein factors involved in gene transcription by interacting with a number of other protein factors. Indeed, PATZ protein, also known as MAZR, ZNF278, or ZSG, is a transcriptional regulatory factor that may function either as activator or as repressor depending upon the cellular context; it has been reported to either activate or repress c-Myc (1, 2), to activate mast cell protease 6 (4), and to repress androgen receptor (5) and CD8 (6) genes.

Different functional and genetic evidences suggest that PATZ might be directly involved in human tumors. Indeed, *PATZ1* is rearranged and deleted in small round cell sarcoma (3), and the chromosomal region where it is located (22q12) is in the human fragile site FRA22B, which suffers loss of heterozygosity in tumors (7). Increased expression of *PATZ1* mRNA has been observed in human malignant neoplasias, including colorectal (8), breast (9), and testicular (10) tumors. Moreover, PATZ knockdown by siRNA either blocks the growth or induces apoptosis of cell lines derived from colorectal cancer or gliomas, respectively (8, 11). However, in testicular tumors alone, PATZ protein expression has been analyzed,

demonstrating that it was mislocalized to cytoplasm (10, 12). Therefore, although *PATZ1* is strongly suggested to be a cancer-related gene, its role as tumor suppressor or oncogene is still controversial.

In the present study, starting from a yeast two-hybrid screening using *PATZ1* full-length cDNA as bait, we demonstrate that PATZ associates with BCL6,[3] a protein that shares with PATZ the N-terminal POZ domain, responsible for such association, and is involved in B and T cell development and lymphomagenesis (13–15, 38). We show that PATZ participates in BCL6 function by enhancing its activity of transcriptional repressor on BCL6 promoter in GC-derived lymphoma B cells. We also show that the knock-down of PATZ in mice causes BCL6-expressing thymus B cell hyperplasias (that eventually lead to B cell lymphomas), in which BCL6 is critical for their onset. The development of BCL6-expressing lymphomas in *Patz1* knock-down mice indicates a potential haploinsufficient tumor suppressor role for the *PATZ1* gene, whose disruption may lead to the lymphomas by activating the BCL6 pathway.

## EXPERIMENTAL PROCEDURES

*Two-hybrid Analysis*—Two-hybrid screens were performed in yeast using full-length *PATZ1* (isoform 4) cDNA as a bait. Human heart and placenta cDNA libraries (Clontech) were simultaneously analyzed. A total of about $2 \times 10^6$ clones were tested for each library, and the specificity of interaction was assessed as described previously (16).

*Plasmids*—Full-length and truncated (devoid of the BTB/POZ domain) cDNAs for the human PATZ protein (isoform 4), Myc-tagged at their 3′-end, were subcloned into the XbaI-HindIII sites of the pcDNA3.1 plasmid (Invitrogen). The cDNA for the human BCL6 protein was subcloned into the EcoRI site of the pCEFL-HA vector (17), in-frame with the upstream HA tag. The BCL6i-luc reporter construct was obtained by cloning the $-4.9$ to $+2.0$-kb fragment of the BCL6 promoter into the pGL3Basic vector as described previously (18).

*Protein Extraction, Immunoprecipitation, and Immunoblot Analysis*—Tissues and cells were lysed in buffer containing 1% Nonidet P-40, 1 mmol/liter EDTA, 50 mmol/liter Tris-HCl (pH 7.5), and 150 mmol/liter NaCl supplemented with Complete protease inhibitors (Roche Applied Science). Total proteins were immunoprecipitated, in the presence or absence of 100 ng/ml ethidium bromide, as described previously (19), or they were directly resolved in a 10% polyacrylamide gel under denaturing conditions and transferred to nitrocellulose filters for Western blot analyses. Membranes were blocked with 5% BSA in TBS and incubated with the primary antibodies. The antibodies used were: anti-HA (sc-805), anti-Myc (sc-40), anti-BCL6 (sc-858), anti-tubulin (sc-5546), anti-vinculin (sc-7649) (Santa Cruz Biotechnology, Santa Cruz, CA), and anti-PATZ (polyclonal antibody raised against a conserved peptide recognizing all PATZ isoforms of mouse and human origin).

*Cell Cultures and Transcriptional Activity Assays*—Raji cells, originally derived from a Burkitt lymphoma, were cultured in RPMI 1640 medium adjusted to contain 1.5 g/liter sodium bicarbonate, 4.5 g/liter glucose, 10 mM HEPES, 1.0 mM sodium pyruvate, penicillin/streptomycin (Invitrogen/Life Technologies Italia, Monza, Italy), and 10% FBS (JRH Biosciences, Lenexa, KS). They were transfected by using the Amaxa Nucleofector kit V (Lonza, Cologne, Germany) following the manufacturer's instructions. COS-1 cells were cultured in DMEM with 10% FBS (JRH Biosciences). They were transfected using Lipofectamine Plus reagents (Invitrogen/Life Technologies Italia) according to the manufacturer's instructions and harvested 42 h after transfection. Cell lysates were extracted as described below and analyzed for luciferase activity. For transcriptional activity assays, a total of $2 \times 10^6$ cells (Raji) were seeded into each well of a 12-well plate and transiently transfected with 4 μg of BCL6i-luc, 5 μg of HA-BCL6, and 0.25–0.5 μg of PATZ-Myc, together with 1 μg of *Renilla* and various amounts of the backbone vectors to keep the total DNA concentration constant. Transfection efficiency, normalized for *Renilla* expression, was assayed with the Dual-Luciferase system (Promega Corp., Madison, WI). All transfection experiments were repeated at least three times. Aliquots of the same lysates were resolved by SDS-PAGE, transferred to nitrocellulose, and immunoblotted with anti-BCL6, anti-PATZ, and anti-vinculin antibodies, as above described.

*Chromatin Immunoprecipitation*—Chromatin immunoprecipitation (ChIP) of Raji cells ($\sim3 \times 10^7$) or chopped spleens ($\sim1$ mg) from *Patz1$^{+/+}$*, *Patz1$^{+/-}$*, and *Patz1$^{-/-}$* mice was carried out with an acetyl-histone H3 immunoprecipitation assay kit (Upstate Biotech Millipore, Lake Placid, NY) according to the manufacturer's instructions (19). The antibodies used are described above. Input DNA and immunoprecipitated DNA were analyzed by standard PCR for the presence of *BCL6* exon 1 and lipoprotein lipase *(LPL)* promoter sequences using the following primers: BCL6 exon 1, forward, 5′-CTCTTACT-CGCCTCTCTAAC-3′; BCL6 exon 1, reverse, 5′-CGGCGGC-AGCAACAGCAATAATCAC-3′; LPL pr, forward, 5′-ACC-AAAGTGTCAAGGGCAAC-3′; and LPL pr, reverse, 5′-ATTCCCTAAACCCAGCATCC-3′.

We also used real-time quantitative PCR to amplify the *BCL6* exon 1, as described below. Primers specific for the glyceraldehyde-3-phosphate dehydrogenase *(GAPDH)* gene were used for normalization of real-time quantitative PCR data. The following primers were used: qBcl6 exon 1, forward, 5′-TAACACCACAA-ACTTGCAAAAGG-3′; qBcl6 exon 1, reverse, 5′-CTCCTCGA-GCTAAATACACAAAAG-3′; qGapdh pr, forward, 5′-TGA-GTCCTATCCTGGGAACCATCA-3′; qGapdh pr, reverse, 5′-TTTGAAATGTGCACGCACCAAGCG-3′.

*Generation of Patz1-Knock-out Mice*—The *Patz1* gene targeting vector was derived from a λΦXII phage library of a 129SvJ mouse strain (Stratagene, La Jolla, CA). It was designed to delete a 2317-bp PstI-XhoI fragment, including the start codon, the coding regions for the POZ domain, the AT-hook, and the first four zinc fingers. It was constructed by subcloning the 5′-flanking region (the SpeI-PstI 3-kb fragment), the *neo* cassette, and the 3′-flanking region (the XhoI-XbaI 3.2-kb fragment) into the Bluescript plasmid (Stratagene) that contained a PacI digestion site inserted at a distance from the multicloning site. The targeting vector was linearized with PacI before electroporation into embryonic stem (ES) cells (Incyte Genomics,
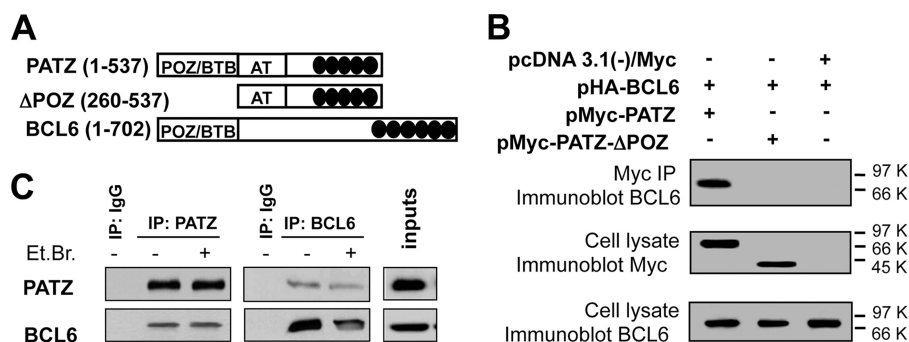
---

FIGURE 1. **Interaction between PATZ and BCL6.** *A*, schematic representation of portions of PATZ and BCL6 encoded by the transfected expression vectors. *AT*, AT-hook domain; *black ovals*, zinc finger motifs. *B*, co-immunoprecipitation (*IP*) of transfected PATZ-Myc, PATZ-ΔPOZ-Myc, and HA-BCL6 proteins in COS-1 cells. *C*, reciprocal co-immunoprecipitation of endogenous PATZ and BCL6 in Raji cells. Immunoprecipitation in the presence of EtBr was performed to control that it was not mediated by contaminating DNA. Immunoprecipitation with nonspecific IgG was carried out as a control for the specificity of the interaction.

Palo Alto, CA). Among 700 G418-resistant ES clones examined, 10 (1.4%) underwent homologous recombination. Two correctly targeted ES cell lines were injected into C57Bl/6J blastocysts. Both ES cell lines gave rise to germ line chimeras that were backcrossed to C57Bl/6J females to obtain *Patz1* heterozygous offspring. For Southern blot analysis, tail DNA samples were digested with StuI and probed with an external 5′ genomic fragment that would detect 9.3- or 8-kb fragments, corresponding to the wild-type and mutant alleles, respectively. The mice were maintained under specific pathogen-free conditions, and all studies were conducted in accordance with Italian regulations for experimentations on animals.

*Isolation of mRNA and Quantitative RT-PCR*—Total RNA was extracted using TRI-reagent solution (Sigma) according to the manufacturer's protocol, treated with DNase I (Invitrogen/Life Technologies Italia), and reverse-transcribed using random hexanucleotides as primers and MuLV reverse transcriptase (PerkinElmer Life Sciences) following the manufacturer's instructions. For quantitative RT-PCR, each reaction was performed three times in triplicate using the SYBR Green PCR master mix (Applied Biosystems, Foster City, CA) under the following conditions: 10 min at 95 °C followed by 40 cycles (15 s at 95 °C and 1 min at 60 °C). Subsequently, a dissociation curve was run to verify amplification specificity. The $2^{-\Delta\Delta CT}$ method was used to calculate relative expression levels (20). Primers specific for the glucose-6-phosphate dehydrogenase (*G6PD*) gene were used for normalization of real-time quantitative PCR data. The following primers were used: Patz, forward, 5′-GAG-CTTCCCCGAGCTCAT-3′; Patz, reverse, 5′-CAGATCTCG-ATGACCGACCT-3′; G6pd, forward, 5′-CAGCGGCAACTA-AACTCAGA-3′; G6pd, reverse, 5′-TTCCCTCAGGA-TCCCACAC-3′.

*Histology and Immunohistochemistry*—Dissected tissues were fixed in 10% formalin and embedded in paraffin by standard procedures. Mounted sections (5 μm thick) were stained with hematoxylin and eosin or incubated in a 750-watt microwave oven for 15 min in EDTA (10 mM, ph 8.0) and processed for immunohistochemistry using the avidin-biotin-peroxidase LSAB+ kit (Dako, Glostrup, Denmark). Endogenous peroxidase was quenched by incubation in 0.1% sodium azide with 0.3% hydrogen peroxide for 30 min at room temperature. Nonspecific binding was blocked by incubation with nonimmune serum. The antisera were directed toward B220 (RA3-6B2;

SouthernBiotech, Birmingham, AL), CD3 (ab5690; Abcam, Cambridge, UK), CD79a (ab3121; Abcam), BCL6 (sc-858; Santa Cruz Biotechnology), and PATZ (described above).

*IgH Gene Rearrangement Analysis*—Genomic DNA was isolated from tumor masses or normal tissues from control mice, and Southern blotting was performed with the $^{32}$P-labeled DNA probe PJ3 representing the $J_H4$ region of the IgH locus (21). A 1.3-kb Pst-1 fragment from the *Gapdh* gene was used for loading control.

*Analysis of Lymphocyte Cell Surface Antigens*—Spleens and thymi removed from mice were dissociated into single cells and stained for FACS analysis on a FACSCalibur flow cytometer (BD Biosciences, Buccinasco, Italy) as described previously (22). All the antibodies used were obtained from Pharmingen.

*Statistical Analyses*—Kaplan-Meyer survival curves were used to analyze the percentage of tumor-free mice. Differences were analyzed by the log rank test. The one-way analysis of variance followed by Tukey's multiple comparison test was used to compare groups of experiments. The statistical significant difference was considered when the *p* value was <0.05.

## RESULTS

*PATZ Interacts with BCL6*—To identify PATZ interacting proteins, two-hybrid screenings of human heart and placenta pretransformed libraries were performed. A total of 87 positive clones (61 and 26 from heart and placenta, respectively) were isolated. Fourteen clones from heart and two from placenta libraries contained most of the coding sequence of the *BCL6* gene (data not shown). To confirm the interaction between PATZ and BCL6 in mammalian cells, co-immunoprecipitation experiments were performed. To this aim, total cell extracts from COS-1 cells transiently transfected with constructs encoding Myc-tagged PATZ, Myc-tagged PATZ-ΔPOZ (devoid of the BTB/POZ domain), and HA-tagged BCL6 (Fig. 1*A*) were subjected to immunoprecipitation using anti-Myc antibody. As shown in Fig. 1*B*, co-precipitation of the BCL6 protein was observed when constructs for BCL6 and full-length PATZ were co-transfected, and not when BCL6 was transfected together with PATZ-ΔPOZ or with the backbone vector. Therefore, PATZ and BCL6 form a complex in mammalian cells, and the POZ domain of PATZ is necessary for such interaction.

FIGURE 2. **Role of PATZ on BCL6 promoter.** *A*, ChIP analysis performed on Raji cells using specific anti-PATZ and anti-BCL6 polyclonal antibodies to detect the endogenous *in vivo* binding of PATZ and BCL6 to exon 1 of BCL6. The recovered DNA was used as a template for PCR with primers that specifically amplify exon 1 of *BCL6* or the promoter region of the *LPL* gene (negative control). *input* indicates PCR products with chromosomal DNA without immunoprecipitation. Nonspecific IgG was used as a negative control. *B*, ChIP assay, revealed by quantitative PCR, on spleens from *Patz1*$^{+/+}$ and *Patz1*$^{-/-}$ mice to detect the binding of PATZ and BCL6 proteins to exon 1 of *Bcl6* DNA. The percentage of immunoprecipitated DNA with respect to the input is reported. *C*, luciferase activity of the BCL6 promoter ($-4.9$ to $+2.0$ kb) in Raji cells. Where indicated, 0.25 and 0.5 $\mu$g of PATZ and/or 5 $\mu$g of BCL6 expression vectors were co-transfected with the BCL6i-luc plasmid. Where required, backbone vectors were also transfected to reach the same total amount of DNA for each experimental point. Data express mean $\pm$ S.D. of three independent experiments. *Asterisks* indicate the statistical results of a multiple comparison test *versus* promoter basic activity. *, $p < 0.05$; **, $p < 0.01$, ***, $p < 0.001$. *D*, representative Western blot analysis to detect BCL6 expression in Raji cells transfected or not with increasing amounts of PATZ expression plasmid, as in *C*. As a control for equal loading, the same blot was incubated with antibodies against vinculin. *E*, Western blot analysis of BCL6 expression in mouse embryonic fibroblasts from Patz1$^{+/+}$ and Patz1$^{-/-}$ mice. Vinculin has been analyzed as a loading control.

Next, to ensure that the interaction between PATZ and BCL6 takes place in a physiological context, endogenous PATZ and BCL6 were co-immunoprecipitated in Raji cells, deriving from a Burkitt lymphoma, which is a GC-derived lymphoma expressing both proteins. The result, shown in Fig. 1*C*, further demonstrates that PATZ and BCL6 interact *in vivo*.

*PATZ Is Involved in BCL6 Negative Autoregulation*—To study the functional consequences of the interaction between PATZ and BCL6, we investigated whether PATZ and BCL6 associate on a BCL6 endogenous target promoter. Previous experiments demonstrated that the *BCL6* gene contains two non-STAT6 functional BCL6 binding sites located within exon 1 (23). Thus, we examined whether PATZ could bind exon 1 of the *BCL6* gene *in vivo*. Endogenous PATZ and BCL6 bind to exon 1 of *BCL6*, as determined by ChIP experiments in Raji cells (Fig. 2*A*). This result was further confirmed *in vivo* using mouse spleens, a tissue that harbors GC cells, where both PATZ and BCL6 proteins were immunoprecipitated on BCL6 exon 1 (Fig. 2*B*). Interestingly, BCL6 binding to its own promoter was enhanced (Fig. 2*B*) in spleens lacking PATZ (obtained from *Patz1* knock-out mice described below). The absence of immunoprecipitated PATZ in Patz1-null tissues confirmed the binding of PATZ to BCL6 exon 1 observed in the wild-type mice.

It is known that BCL6, by binding to its exon 1 and recruiting the distal *cis*-acting factor ZEB1, represses its own transcription, thus establishing a circuit of negative autoregulation (23,

24). To further investigate the role of PATZ in such a function of BCL6, we used a reporter construct driving luciferase gene expression under control of a BCL6 genomic sequence of 6.9 kb, including the ZEB1-responsive element, exon 1, and 1.5 kb of intron 1 (BCL6i-luc) (18). Raji cells were co-transfected with BCL6i-luc and plasmids expressing PATZ, BCL6, or both proteins (Fig. 2*C*). As expected, BCL6 expression resulted in downregulation of the BCL6 promoter activity. A similar, but less strong, activity was also achieved by PATZ, leading to a dose-dependent repression of this BCL6 promoter region. Interestingly, PATZ and BCL6 co-transfection resulted in the enhancement of the BCL6-dependent repression (Fig. 2*C*). Western blot analysis of Raji cells transfected or not with increasing amounts of PATZ expression plasmid, as in Fig. 2*C*, confirmed the negative dose-dependent effect of PATZ on BCL6 expression (Fig. 2*D*). To finally assess the dependence of BCL6 expression from PATZ, we analyzed, by Western blot, the BCL6 protein levels in mouse embryonic fibroblasts from Patz1$^{+/+}$ and Patz1$^{-/-}$ mice (described below). As shown in Fig. 2*E*, Patz1-null mouse embryonic fibroblasts showed a significant increase in BCL6 expression, which confirms the negative regulatory role of PATZ on it.

*Disruption of Mouse Patz1 Gene Causes Thymus B Cell Expansion, Which Eventually Leads to B Cell Lymphomas*—To gain insights into the physiological role of PATZ *in vivo*, a targeting vector was designed to knock out the mouse *Patz1* gene
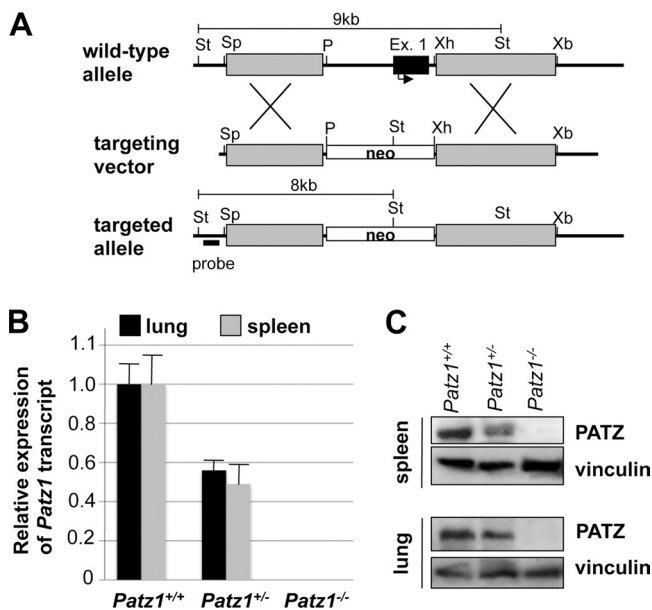
FIGURE 3. **Generation of *Patz1* knock-out mice.** *A*, schematic representation of the wild-type and mutant alleles and the targeting vector. *St*, StuI; *Sp*, SpeI; *P*, PstI; *Ex.*, exon; *Xb*, XbaI. *B* and *C*, quantitative RT-PCR (*B*) and Western blot analysis (*C*) in tissues from *Patz1*⁺/⁺, *Patz1*⁺/⁻, and *Patz1*⁻/⁻ mice, to detect PATZ expression and confirm its knock-out at both RNA and protein levels. Data express mean ± S.D. of three independent experiments.

by homologous recombination in ES cells (Fig. 3*A*). Inactivation of the *Patz1* allele was verified by analyzing *Patz1* expression in adult tissues using quantitative RT-PCR and Western blot (Fig. 3, *B* and *C*). As expected, *Patz1* mRNA and protein were undetectable in homozygous mutants, whereas they were present at about half-levels in heterozygous as compared with wild-type controls. Heterozygous mice were viable and fertile, but heterozygous intercrosses produced viable homozygous mutants at non-Mendelian frequencies. Indeed, the large majority of homozygous mutants (about 75% on average) died prenatally due to developmental defects in the cardiac outflow tract.[4] Here we focused on some phenotypes, observed in adult mice (both heterozygous and homozygous for the *Patz1*-null mutation), which can be due to an impaired regulation of the *BCL6* gene.

By 2–3 months of age, with a similar frequency (75%), Patz1⁺/⁻ and Patz1⁻/⁻ mice develop thymus hyperplasias characterized by focal expansion of an intramedullary B cell population (Fig. 4*A*). B cells are the minority cell type (0.82 ± 0.50%) in the thymus of wild-type animals, as confirmed by FACS analysis in a cohort of 20 animals, but significantly increase to an average of 5.94 ± 4.42 ($p < 0.05$) in an equal number of *Patz1*⁺/⁻ mice (Fig. 4*B*). A similar increase of B cells was also observed in Patz1⁻/⁻, where, for the limited number of available animals, we could only do a qualitative analysis (data not shown). To exclude that this B cell expansion could be due to formation of intrathymic reactive B cell follicles possibly induced by an altered CD4 helper *versus* cytotoxic subset ratio (25), we analyzed CD4+ and CD8+ lymphocyte populations by FACS in *Patz1*⁺/⁻ thymi showing B cell hyperplasia, without

finding any differences in comparison with wild-type controls (data not shown). Interestingly, in 4 out of 75 Patz1⁺/⁻ mice sacrificed at an advanced age (17–22 months old), we also found thymus B cell lymphomas, characterized by large cells with marked cell-to-cell variation in size and shape and abundant pale cytoplasm, which were diagnosed as diffuse large B cell lymphomas by our pathologists (Fig. 4*C* and data not shown).

*Thymus B Cell Lesions in Patz1 Knock-out Mice Are Dependent on Bcl6 Expression*—Pathological thymus B cells are considered to originate from the GC (26). Accordingly, focal expression of BCL6 was detected in *Patz1*-knock-out thymus lesions (either hyperplasia or lymphomas) but was absent in the wild-type controls (Fig. 5*A*). Western blot analyses on thymus tissues from *Patz1*⁺/⁻ mice confirmed the expression of BCL6, which was absent in *Patz1*⁺/⁺ controls (Fig. 5*B*). Up-regulation of BCL6 in these cells is consistent with the role of PATZ in BCL6 autoregulation (see above), which leads us to suggest that decreased or null levels of PATZ causes up-regulation of BCL6 expression, which in turn could be responsible for the thymus pathological phenotype. To validate our hypothesis of a role for increased BCL6 expression in the development of certain phenotypes in *Patz1* knock-out mice, we crossed *Patz1*⁺/⁻ with *Bcl6*⁺/⁻ mice (27) to generate double mutants. *Patz1*⁻/⁻; *Bcl6*⁺/⁺, *Patz1*⁺/⁺;*Bcl6*⁻/⁻, and *Patz1*⁻/⁻;*Bcl6*⁻/⁻ mice died during embryogenesis. However, because we observed the thymus phenotype in *Patz1* heterozygous mice, we analyzed the alterations present in *Patz1*⁺/⁻;*Bcl6*⁺/⁺ mice and compared them with the double heterozygous *Patz1/Bcl6* mutants.

Cohorts of 10 *Patz1*⁺/⁻;*Bcl6*⁺/⁺ and 10 *Patz1*⁺/⁻;*Bcl6*⁺/⁻ mice were equally distributed by gender and sacrificed at 12 months of age. Their thymus was analyzed by histological, immunohistochemical, and FACS assays. As shown in Fig. 5*C*, where representative FACS analyses are shown, 100% of the *Patz1*⁺/⁻;*Bcl6*⁺/⁻ mice analyzed did not show any significant thymus B cell expansion as compared with the *Patz1*⁺/⁻; *Bcl6*⁺/⁺ controls. Immunohistochemical analyses confirmed this result in 80% of the cases, whereas in the remaining 20% of double heterozygous mice, an aberrant thymus B cell hyperplasia was observed, but it was strongly reduced as compared with that observed in *Patz1*⁺/⁻;*Bcl6*⁺/⁺ mice (Fig. 5*D*). These results confirm a key role for the up-regulation of BCL6 in the pathological thymus phenotype of *Patz1* knock-out mice.

*Increased Tumorigenesis in Patz1 Knock-out Mice*—Although initially healthy, many adult *Patz1*⁺/⁻ and most of the few available *Patz1*⁻/⁻ mice developed signs of morbidity and displayed visible tumors as they aged. As evident in the survival curves in Fig. 6*A*, *Patz1*⁻/⁻ and *Patz1*⁺/⁻ mice showed an increased incidence of neoplastic lesions at ~17 or 21 months of age, respectively. Only 12% of the *Patz1*⁻/⁻ and 67% of the *Patz1*⁺/⁻ animals were tumor-free at 20 months, in contrast to the 95% of wild-type mice that were tumor-free at the same age.

The histological analyses revealed that 43 of 75 (57%) *Patz1*⁺/⁻ and 9 of 11 (82%) *Patz1*⁻/⁻ mice developed malignant tumors, *versus* only 7 of 63 (11%) wild-type mice. *Patz1* knock-out tumors were mainly lymphomas, but hepatocellular carcinomas and rare sarcomas and lung adenocarcinomas were also detected. Wild-type animals developed lymphomas and

---

[4] T. Valentino, D. Palmieri, M. Vitiello, A. Simeone, G. Palma, C. Arra, P. Chieffi, L. Chiariotti, A. Fusco, and M. Fedele, manuscript submitted.
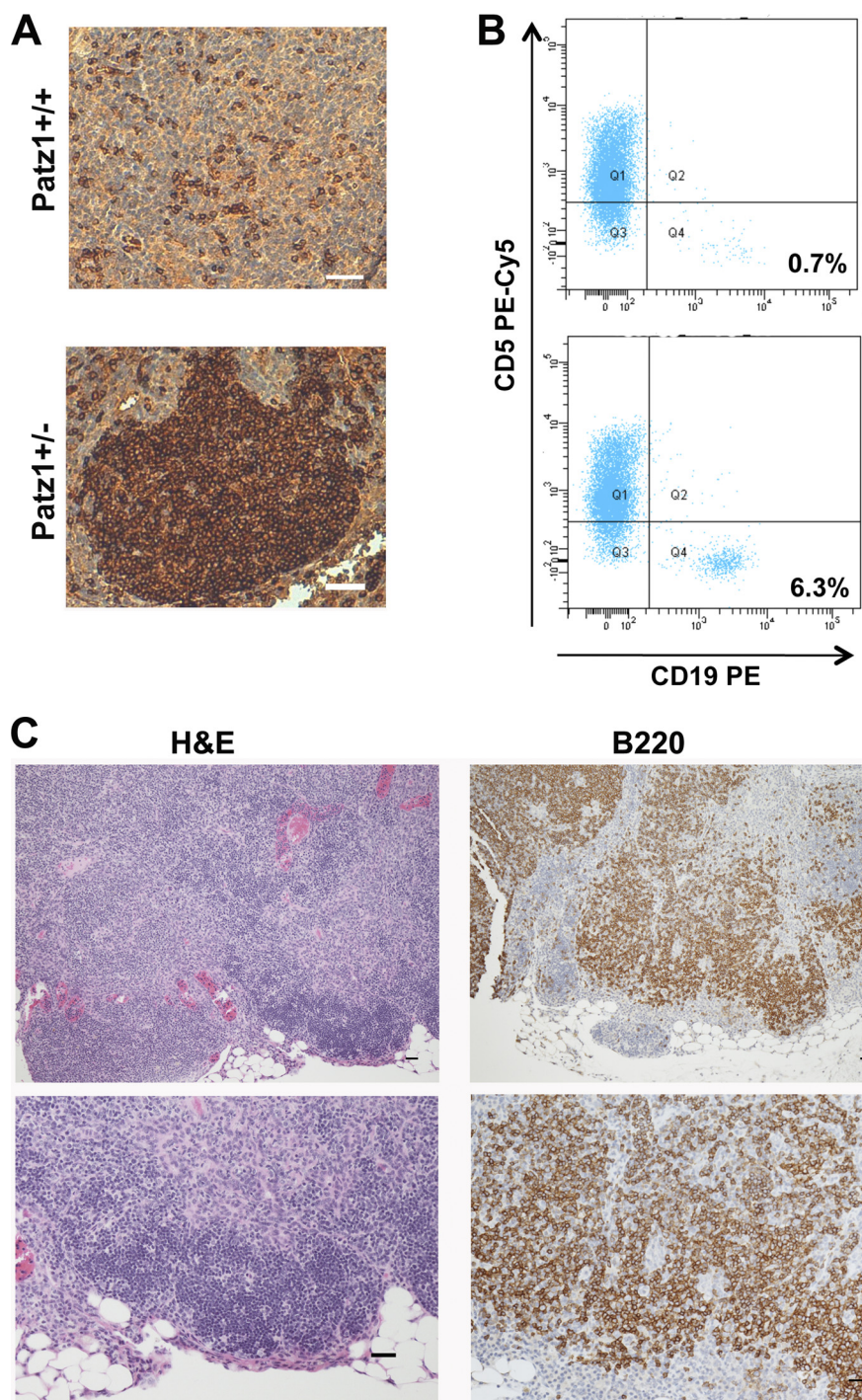
FIGURE 4. **Thymus neoplasias in *Patz1* knock-out mice.** *A*, immunohistochemical analysis in representative thymus sections of *Patz1*^{+/+} and *Patz1*^{+/−} mice. B220 staining shows the presence of a focal B cell hyperplasia in the medulla of the mutant sample, whereas only scattered B cells were present in the wild-type control. *Scale bars*, 100 $\mu$m. *B*, flow cytometry dot blots of the thymi showed in B stained with CD19 and CD5 antibodies. A distinct population of cells that positively stains with CD19-PE antibody in the *Patz1*^{+/−} (*lower panel*) is evident. No appreciable CD19+ cell population was found in the wild-type control (*upper panel*). For each analysis, 10,000 events were counted. The relative percentage of CD19$^+$ cells (B lymphocytes) was indicated in the *right-bottom corner* of each dot plot. *PE*, Phycoerythrin. *C*, representative sample of a thymus B cell lymphoma developed by a *Patz1*^{+/−} mouse. *Left panels*, hematoxylin and eosin staining; *right panels*, immunostaining for B220. *Scale bars*, 100 $\mu$m.

one hepatocellular carcinoma (Fig. 6*B* and data not shown). Lymphomas from wild-type mice were all of the B cell lineage but did not show BCL6 expression nor PATZ down-regulation as compared with normal controls (data not shown).

To determine whether the tumors in Patz1^{+/−} mice occurred via loss of heterozygosity or haploinsufficiency, PATZ protein expression and *Patz1* gene sequence were analyzed in the tumor tissues from *Patz1*^{+/−} mice. Western blot (Fig. 6*C*) and immunohistochemical analysis (data not shown) revealed that PATZ was present in all of the tumors examined. Furthermore, sequence analysis of *Patz1* cDNA isolated from eight *Patz1*^{+/−} tumors showed no mutation or rearrangement (data
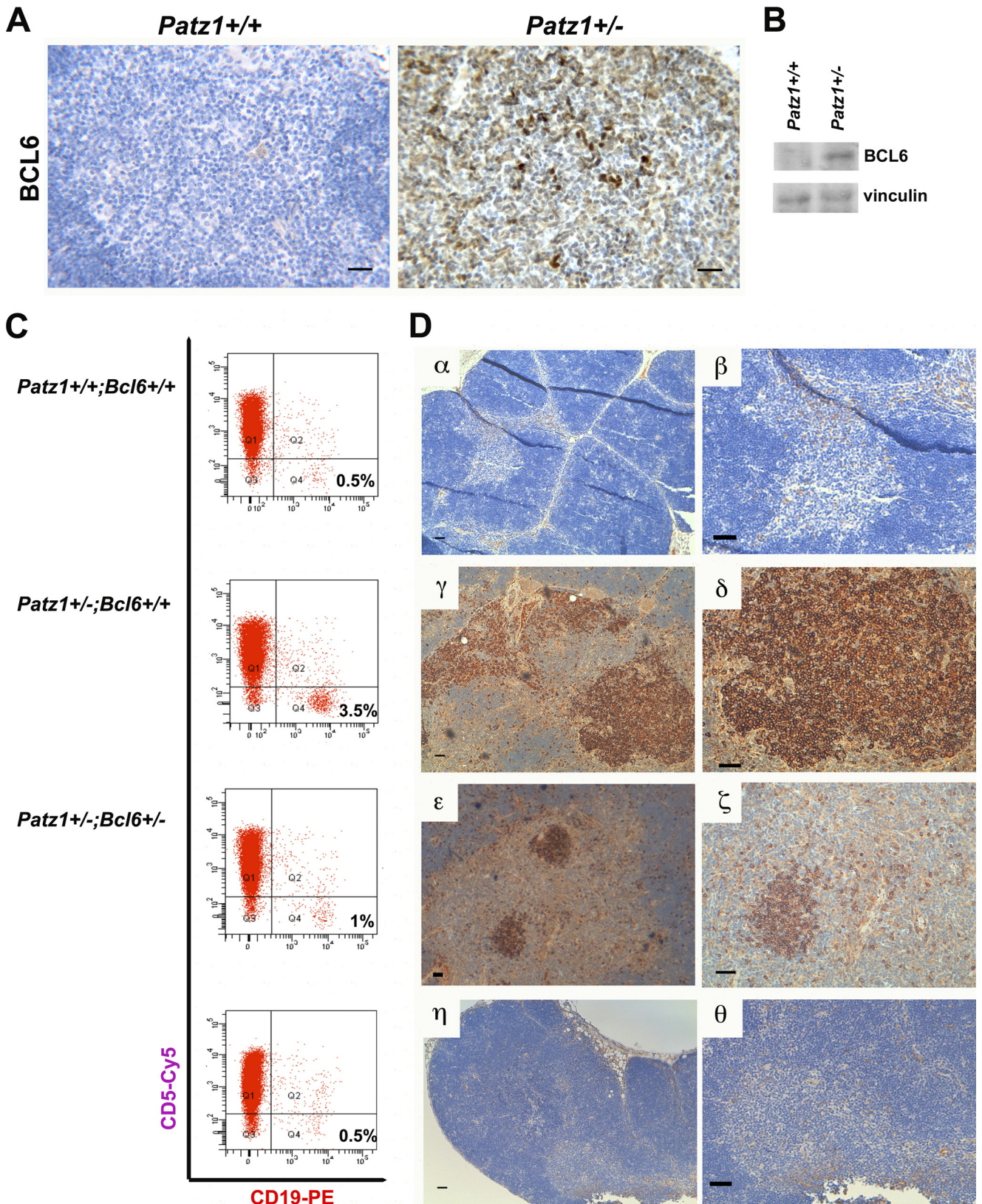
FIGURE 5. **Key role of BCL6 in thymus B cell expansion of *Patz1* knock-out mice.** *A*, immunohistochemical staining of BCL6 in representative thymus samples from *Patz1*^{+/+} (*left panel*) and *Patz1*^{+/−} (*right panel*) mice. *Scale bar*, 100 $\mu$m. *B*, Western blot analysis for BCL6 expression in a pool of three *Patz1*^{+/+} and three *Patz1*^{+/−} thymi. *C*, flow cytometry of representative thymi from *Patz1*^{+/+};*Bcl6*^{+/+}, *Patz1*^{+/−};*Bcl6*^{+/+}, and *Patz1*^{+/−};*Bcl6*^{+/−} mice. The thymocytes were double-stained for specific B (CD19) and T cell (CD5) surface antigens. For each analysis, 10,000 events were counted. The relative percentage of CD19^{+} cells (B lymphocytes) was indicated in the *right-bottom corner* of each dot plot. *CD19-PE*, CD19-Phycoerythrin staining. *D*, immunohistochemical analysis of the thymi shown in *C* to detect B cells (stained with anti-B220). Only scattered positive cells were detected in *Patz1*^{+/+};*Bcl6*^{+/+} ($\alpha$,$\beta$) and most *Patz1*^{+/−};*Bcl6*^{+/−} thymi ($\eta$,$\theta$). Large focal hyperplasias of B cells were detected in *Patz1*^{+/−};*Bcl6*^{+/+} ($\gamma$, $\delta$) thymi, and small focal positivity was detected in some *Patz1*^{+/−};*Bcl6*^{+/−} thymi ($\epsilon$, $\zeta$). *Scale bars*, 100 $\mu$m.
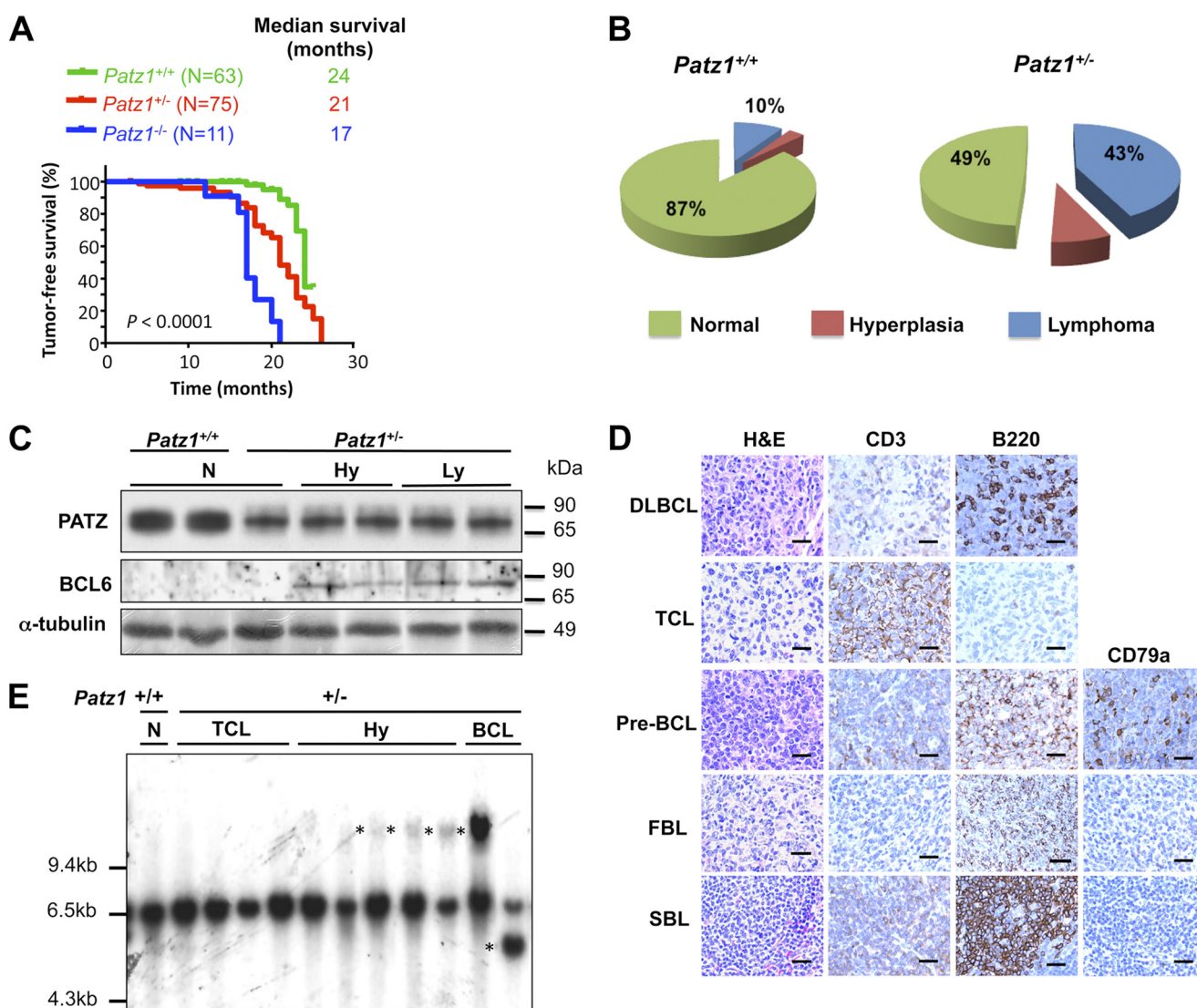
FIGURE 6. **Increased lymphomagenesis in Patz1 knock-out mice.** *A*, Kaplan-Meyer tumor incidence analysis of *Patz1*$^{+/+}$, *Patz1*$^{+/-}$, and *Patz1*$^{-/-}$ mice. Cohorts of 63 wild-type, 75 heterozygous, and 11 homozygous *Patz1* knock-out mice were monitored and harvested when they exhibited symptoms of disease. The curves were significantly different ($p < 0.0001$) as determined by log rank test. *B*, the lymphoid phenotype, as a function of the relative percentage, in mice homozygous and heterozygous for the *Patz1*-null mutation *versus* wild-type controls was plotted as pie charts. The number of mice analyzed for each genotype is the same as in *A*. *C*, Western blot analysis showing expression of BCL6 and PATZ in spleen samples from *Patz1*$^{+/+}$ and *Patz1*$^{+/-}$ mice. α-Tubulin expression was evaluated as a loading control. *N*, normal; *Hy*, hyperplasia; *Ly*, lymphoma. *D*, immunohistochemical staining for the phenotypic characterization of lymphomas in *Patz1*$^{+/-}$ spleen samples. Representative *Patz1*$^{+/-}$ spleen samples of all types of lymphomas observed are shown (for the percentage of each type, see under "Results"). Antibodies used for the staining are indicated on the *top*. *H&E*, hematoxylin and eosin staining; *DLBCL*, diffuse large cell B cell lymphoma; *TCL*, T cell lymphoma; *pre-BCL*, pre-B cell lymphoma; *FBL*, follicular B cell lymphoma; *SBL*, small B cell lymphoma. *Scale bars*, 100 μm. *E*, *IgH* gene rearrangements were analyzed by Southern blot on EcoRI-digested spleen DNA. Control (+/+) is the wild-type mouse with the genomic 6.5-kb fragment representing the gene in its germ line configuration. All hyperplastic (*Hy*) and B cell lymphoma samples from *Patz1*$^{+/-}$ mice, and normal spleen from a *Patz1*$^{-/-}$ mouse, show rearranged extra bands (*asterisks*). The histological diagnoses of the spleens are indicated above.

not shown). These results indicate that haploinsufficiency, rather than loss of heterozygosity, accounts for the tumor occurrence in *Patz1*$^{+/-}$ mice, thus suggesting *Patz1* as a haploinsufficient tumor suppressor gene.

Spleen lymphomas were the most representative malignant diseases in *Patz1* knock-out mice, and they were further characterized to determine the mechanism by which reduced *Patz1* expression induces such neoplasias. Tumor sections from *Patz1*$^{+/-}$ mice were stained with antibodies raised against T cell- and B cell-specific markers to determine the cell type of origin of the lymphoma. Interestingly, we found both B type and T type lymphomas with a prevalence of B (28%) *versus* T lymphomas (17%). The B type lymphoma (BCL) subtypes, as

defined by Morse *et al.* (28), were as follows: (*a*) diffuse large B cell (16.8%), (*b*) follicular B cell (5.6%), (*c*) pre-B cell (2.8%), and (*d*) small B cell lymphomas (2.8%) (Fig. 6D). Flow cytometry analysis confirmed the immunohistochemical data (data not shown). To further characterize lymphoid neoplasias, *IgH* gene configuration was analyzed by Southern blot of EcoRI-digested spleen DNA from *Patz1*$^{+/+}$ and *Patz1*$^{+/-}$ mice using a probe representing the J$_H$4 region of the *IgH* locus (Fig. 6E). The 6.5-kb fragment represents the germ line configuration of the gene. All BCLs showed oligoclonal rearrangements of the germ line *IgH* joining region (Fig. 6E, *asterisks*). Interestingly, benign lymphoproliferative diseases often show aberrant V(D)J recombination at the *IgH* locus, suggesting that they may represent an

early stage in the development of BCLs. The same Southern blot was also probed for *gapdh*, which gave rise to a unique band for all loaded samples (data not shown). Both BCLs and lymphoproliferative diseases expressed BCL6, whereas it was not detectable in wild-type controls or normal spleens from *Patz1* knock-out mice (Fig. 6C), suggesting a key role for this oncoprotein in development of such neoplasias.

## DISCUSSION

Previous studies suggest a cancer-related role for PATZ (3, 8–11), but the mechanisms by which PATZ is involved in the process of carcinogenesis are still controversial. Our data indicate that PATZ acts as a tumor suppressor in lymphomagenesis by inhibiting BCL6 expression. We first showed that PATZ and BCL6 bind to each other. This finding is consistent with the notion that POK proteins, such as PATZ and BCL6, commonly aggregate in large nuclear complexes by self-interaction, as heterodimers with other POK proteins and in association with unrelated partners, such as transcriptional corepressors, as a way to extend the repertoire of their target genes and/or the ways they act on their expression (29). BCL6 is the most commonly altered proto-oncogene in non-Hodgkin lymphomas, the majority of which derive from normal GC B cells (30). In fact, its sustained expression causes malignant transformation of GC B cells (31). Nearly half of human diffuse large B cell lymphomas, the most common form of non-Hodgkin lymphomas, express BCL6 constitutively, mainly as a consequence of *BCL6* gene rearrangements and activating point mutations that target the 5′ regulatory region of this gene (23, 24, 32, 33). However, different studies showed that *BCL6* expression in lymphoma is largely independent from the corresponding chromosomal alterations, suggesting that mechanisms other than gene rearrangements or mutations can deregulate its expression in lymphomas (34, 35). BCL6 expression is tightly regulated in a lineage- and developmental-stage-specific manner, and disruption of normal controls can contribute to lymphomagenesis (13, 14, 36). Transcription of the *BCL6* gene is negatively self-regulated by means of the interaction of two BCL6 binding sites within exon 1 of the gene and the BCL6 protein itself, which is a potent transcription repressor, and both chromosomal translocations and activating mutations allow lymphoma cells to bypass this negative autoregulation mechanism (23, 24). To date, a variety of corepressors have been described. Among them, the CtBP1 and ZEB1 transcriptional repressors are required for BCL6 autoregulation (18, 37). In a recent model, a repressive complex at the BCL6 locus that involves binding of transcription factors to both exon 1 and a distant *cis*-acting element (HSS-4.4) has been suggested to regulate BCL6 transcription. In this complex, ZEB1 and BCL6, which bind to distant sites, are linked through binding of the common corepressor CtBP1 (18). In the present study, we show that PATZ can bind *BCL6* exon 1 and negatively modulate *BCL6* promoter activity. Therefore, we speculate that PATZ can be one of the transcription factors involved in the complex and that, because of its ability to bind the minor groove of DNA via the AT-hooks, could be crucial for the bending of DNA required to put together distant *cis*-acting transcription factors. Because PATZ can interact and cooperate with BCL6, we can suggest that it

acts together with BCL6 in its autoregulation. However, we cannot exclude that PATZ can also act without BCL6, thus contributing to keep BCL6 expression off when BCL6 is not expressed at all. Consistent with a role of PATZ in BCL6 negative regulation, we also show that mice carrying a null mutation of the *Patz1* gene develop an aberrant expansion of thymus B cells, in which BCL6 expression is up-regulated. We believe that this phenotype, which we demonstrated to be dependent on BCL6 expression, is also responsible for the development of BCLs that we observe in both thymi and spleens of Patz1 knock-out mice at a later age.

In conclusion, our data indicate a haploinsufficient tumor suppressor role for PATZ that would act in lymphomagenesis by down-regulating BCL6 expression.

## REFERENCES

1. Fedele, M., Benvenuto, G., Pero, R., Majello, B., Battista, S., Lembo, F., Vollono, E., Day, P. M., Santoro, M., Lania, L., Bruni, C. B., Fusco, A., and Chiariotti, L. (2000) A novel member of the BTB/POZ family, PATZ, associates with the RNF4 RING finger protein and acts as a transcriptional repressor. *J. Biol. Chem.* **275,** 7894–7901
2. Kobayashi, A., Yamagiwa, H., Hoshino, H., Muto, A., Sato, K., Morita, M., Hayashi, N., Yamamoto, M., and Igarashi, K. (2000) A combinatorial code for gene expression generated by transcription factor Bach2 and MAZR (MAZ-related factor) through the BTB/POZ domain. *Mol. Cell Biol.* **20,** 1733–1746
3. Mastrangelo, T., Modena, P., Tornielli, S., Bullrich, F., Testi, M. A., Mezzelani, A., Radice, P., Azzarelli, A., Pilotti, S., Croce, C. M., Pierotti, M. A., and Sozzi, G. (2000) A novel zinc finger gene is fused to EWS in small round cell tumor. *Oncogene* **19,** 3799–37804
4. Morii, E., Oboki, K., Kataoka, T. R., Igarashi, K., and Kitamura, Y. (2002) Interaction and cooperation of *mi* transcription factor (MITF) and myc-associated zinc-finger protein-related factor (MAZR) for transcription of mouse mast cell protease 6 gene. *J. Biol. Chem.* **277,** 8566–8571
5. Pero, R., Lembo, F., Palmieri, E. A., Vitiello, C., Fedele, M., Fusco, A., Bruni, C. B., and Chiariotti, L. (2002) PATZ attenuates the RNF4-mediated enhancement of androgen receptor-dependent transcription. *J. Biol. Chem.* **277,** 3280–3285
6. Bilic, I., Koesters, C., Unger, B., Sekimata, M., Hertweck, A., Maschek, R., Wilson, C. B., and Ellmeier, W. (2006) Negative regulation of CD8 expression via Cd8 enhancer-mediated recruitment of the zinc finger protein MAZR. *Nat. Immunol.* **7,** 392–400
7. Burrow, A. A., Williams, L. E., Pierce, L. C., and Wang, Y. H. (2009) Over half of breakpoints in gene pairs involved in cancer-specific recurrent translocations are mapped to human chromosomal fragile sites. *BMC Genomics* **10,** 59
8. Tian, X., Sun, D., Zhang, Y., Zhao, S., Xiong, H., and Fang, J. (2008) Zinc finger protein 278, a potential oncogene in human colorectal cancer. *Acta Biochim. Biophys. Sin.* **40,** 289–296
9. Yang, W. L., Ravatn, R., Kudoh, K., Alabanza, L., and Chin, K. V. (2010) Interaction of the regulatory subunit of the cAMP-dependent protein kinase with PATZ1 (ZNF278). *Biochem. Biophys. Res. Commun.* **391,** 1318–1323
10. Fedele, M., Franco, R., Salvatore, G., Paronetto, M. P., Barbagallo, F., Pero, R., Chiariotti, L., Sette, C., Tramontano, D., Chieffi, G., Fusco, A., and Chieffi, P. (2008) *PATZ1* gene has a critical role in the spermatogenesis and testicular tumors. *J. Pathol.* **215,** 39–47
11. Tritz, R., Mueller, B. M., Hickey, M. J., Lin, A. H., Gomez, G. G., Hadwiger,

P., Sah, D. W., Muldoon, L., Neuwelt, E. A., and Kruse, C. A. (2008) siRNA down-regulation of the PATZ1 Gene in human glioma cells increases their sensitivity to apoptotic stimuli. *Cancer Ther.* **6,** 865–876

12. Esposito, F., Boscia, F., Franco, R., Tornincasa, M., Fusco, A., Kitazawa, S., Looijenga, L. H., and Chieffi, P. (2011) Down-regulation of estrogen receptor-β associates with transcriptional co-regulator PATZ1 delocalization in human testicular seminomas. *J. Pathol.* **224,** 110–120

13. Pasqualucci, L., Bereschenko, O., Niu, H., Klein, U., Basso, K., Guglielmino, R., Cattoretti, G., and Dalla-Favera, R. (2003) Molecular pathogenesis of non-Hodgkin's lymphoma: the role of Bcl-6. *Leuk. Lymphoma* **44,** S5–S12

14. Ichii, H., Sakamoto, A., Kuroda, Y., and Tokuhisa, T. (2004) Bcl6 acts as an amplifier for the generation and proliferative capacity of central memory CD8$^+$ T cells. *J. Immunol.* **173,** 883–891

15. Cattoretti, G., Pasqualucci, L., Ballon, G., Tam, W., Nandula, S. V., Shen, Q., Mo, T., Murty, V. V., and Dalla-Favera, R. (2005) Deregulated BCL6 expression recapitulates the pathogenesis of human diffuse large B cell lymphomas in mice. *Cancer Cell* **7,** 445–455

16. Lembo, F., Pero, R., Angrisano, T., Vitiello, C., Iuliano, R., Bruni, C. B., and Chiariotti, L. (2003) MBDin, a novel MBD2-interacting protein, relieves MBD2 repression potential and reactivates transcription from methylated promoters. *Mol. Cell Biol.* **23,** 1656–1665

17. Melillo, R. M., Pierantoni, G. M., Scala, S., Battista, S., Fedele, M., Stella, A., De Biasio, M. C., Chiappetta, G., Fidanza, V., Condorelli, G., Santoro, M., Croce, C. M., Viglietto, G., and Fusco, A. (2001) Critical role of the HMGI(Y) proteins in adipocytic cell growth and differentiation. *Mol. Cell Biol.* **21,** 2485–2495

18. Papadopoulou, V., Postigo, A., Sánchez-Tilló, E., Porter, A. C., and Wagner, S. D. (2010) ZEB1 and CtBP form a repressive complex at a distal promoter element of the BCL6 locus. *Biochem. J.* **427,** 541–550

19. Fedele, M., Visone, R., De Martino, I., Troncone, G., Palmieri, D., Battista, S., Ciarmiello, A., Pallante, P., Arra, C., Melillo, R. M., Helin, K., Croce, C. M., and Fusco, A. (2006) HMGA2 induces pituitary tumorigenesis by enhancing E2F1 activity. *Cancer Cell* **9,** 459–471

20. Livak, K. J., and Schmittgen, T. (2001) Analysis of relative gene expression data using real-time quantitative PCR and the $2^{-\Delta\Delta CT}$ method. *Methods* **25,** 402–408

21. Bichi, R., Shinton, S. A., Martin, E. S., Koval, A., Calin, G. A., Cesari, R., Russo, G., Hardy, R. R., and Croce, C. M. (2002) Human chronic lymphocytic leukemia modeled in mouse by targeted TCL1 expression. *Proc. Natl. Acad. Sci. U.S.A.* **99,** 6955–6960

22. Fedele, M., Fidanza, V., Battista, S., Pentimalli, F., Klein-Szanto, A. J., Visone, R., De Martino, I., Curcio, A., Morisco, C., Del Vecchio, L., Baldassarre, G., Arra, C., Viglietto, G., Indolfi, C., Croce, C. M., and Fusco, A. (2006) Haploinsufficiency of the *Hmga1* gene causes cardiac hypertrophy and myelo-lymphoproliferative disorders in mice. *Cancer Res.* **66,** 2536–2543

23. Wang, X., Li, Z., Naganuma, A., and Ye, B. H. (2002) Negative autoregulation of BCL-6 is bypassed by genetic alterations in diffuse large B cell lymphomas. *Proc. Natl. Acad. Sci. U.S.A.* **99,** 15018–15023

24. Pasqualucci, L., Migliazza, A., Basso, K., Houldsworth, J., Chaganti, R. S., and Dalla-Favera, R. (2003) Mutations of the *BCL6* proto-oncogene disrupt its negative autoregulation in diffuse large B-cell lymphoma. *Blood* **101,** 2914–2923

25. Sakaguchi, S., Hombauer, M., Bilic, I., Naoe, Y., Schebesta, A., Taniuchi, I., and Ellmeier, W. (2010) The zinc-finger protein MAZR is part of the transcription factor network that controls the CD4 *versus* CD8 lineage fate of double-positive thymocytes. *Nat. Immunol.* **11,** 442–448

26. Csernus, B., Timár, B., Fülöp, Z., Bognár, A., Szepesi, A., László, T., Jáksó, P., Warnke, R., Kopper, L., and Matolcsy, A. (2004) Mutational analysis of $IgV_H$ and *BCL-6* genes suggests thymic B-cells origin of mediastinal (thymic) B-cell lymphoma. *Leuk. Lymphoma* **45,** 2105–2110

27. Ye, B. H., Cattoretti, G., Shen, Q., Zhang, J., Hawe, N., de Waard, R., Leung, C., Nouri-Shirazi, M., Orazi, A., Chaganti, R. S., Rothman, P., Stall, A. M., Pandolfi, P. P., and Dalla-Favera, R. (1997) The *BCL-6* proto-oncogene controls germinal-center formation and Th2-type inflammation. *Nat. Genet.* **16,** 161–170

28. Morse, H. C., 3rd, Anver, M. R., Fredrickson, T. N., Haines, D. C., Harris, A. W., Harris, N. L., Jaffe, E. S., Kogan, S. C., MacLennan, I. C., Pattengale, P. K., and Ward, J. M. (2002) Bethesda proposals for classification of lymphoid neoplasms in mice. *Blood* **100,** 246–258

29. Davies, J. M., Hawe, N., Kabarowski, J., Huang, Q. H., Zhu, J., Brand, N. J., Leprince, D., Dhordain, P., Cook, M., Morriss-Kay, G., and Zelent, A. (1999) Novel BTB/POZ domain zinc-finger protein, LRF, is a potential target of the *LAZ-3/BCL-6* oncogene. *Oncogene* **18,** 365–375

30. Fearon, D. T., Manders, P., and Wagner, S. D. (2001) Arrested differentiation, the self-renewing memory lymphocyte, and vaccination. *Science* **293,** 248–250

31. Ci, W., Polo, J. M., Cerchietti, L., Shaknovich, R., Wang, L., Yang, S. N., Ye, K., Farinha, P., Horsman, D. E., Gascoyne, R. D., Elemento, O., and Melnick, A. (2009) The BCL6 transcriptional program features repression of multiple oncogenes in primary B cells and is deregulated in DLBCL. *Blood* **113,** 5536–5548

32. Ye, B. H., Chaganti, S., Chang, C. C., Niu, H., Corradini, P., Chaganti, R. S., and Dalla-Favera, R. (1995) Chromosomal translocations cause deregulated BCL6 expression by promoter substitution in B cell lymphoma. *EMBO J.* **14,** 6209–6217

33. Lo Coco, F., Ye, B. H., Lista, F., Corradini, P., Offit, K., Knowles, D. M., Chaganti, R. S., and Dalla-Favera, R. (1994) Rearrangements of the *BCL6* gene in diffuse large cell non-Hodgkin's lymphoma. *Blood* **83,** 1757–1759

34. Muramatsu, M., Akasaka, T., Kadowaki, N., Ohno, H., Fukuhara, S., and Okuma, M. (1997) Rearrangement of the *BCL6* gene in B-cell lymphoid neoplasms. *Leukemia* **11,** 318–320

35. Skinnider, B. F., Horsman, D. E., Dupuis, B., and Gascoyne, R. D. (1999) Bcl-6 and Bcl-2 protein expression in diffuse large B-cell lymphoma and follicular lymphoma: correlation with 3q27 and 18q21 chromosomal abnormalities. *Hum. Pathol.* **30,** 803–808

36. Saito, M., Gao, J., Basso, K., Kitagawa, Y., Smith, P. M., Bhagat, G., Pernis, A., Pasqualucci, L., and Dalla-Favera, R. (2007) A signaling pathway mediating down-regulation of *BCL6* in germinal center B cells is blocked by *BCL6* gene alterations in B cell lymphoma. *Cancer Cell* **12,** 280–292

37. Mendez, L. M., Polo, J. M., Yu, J. J., Krupski, M., Ding, B. B., Melnick, A., Ye, B. H. (2008) CtBP is an essential corepressor for BCL6 autoregulation. *Mol. Cell Biol.* **28,** 2175–2186

38. Dent, A. L., Shaffer, A. L., Yu, X., Allman, D., and Staudt, L. M. (1997) Control of inflammation, cytokine expression, and germinal center formation by BCL-6. *Science* **276,** 589–592
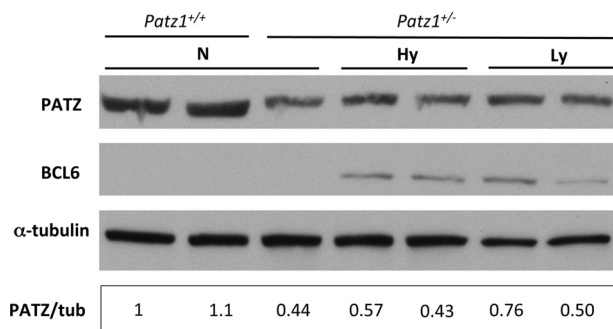
# ADDITIONS AND CORRECTIONS

## POZ-, AT-hook-, and zinc finger-containing protein (PATZ) interacts with human oncogene B cell lymphoma 6 (BCL6) and is required for its negative autoregulation.

Raffaela Pero, Dario Palmieri, Tiziana Angrisano, Teresa Valentino, Antonella Federico, Renato Franco, Francesca Lembo, Andres J. Klein-Szanto, Luigi Del Vecchio, Donatella Montanaro, Simona Keller, Claudio Arra, Vasiliki Papadopoulou, Simon D. Wagner, Carlo M. Croce, Alfredo Fusco, Lorenzo Chiariotti, and Monica Fedele

PAGE 18315:

Western blot images representing PATZ, BCL6, and tubulin in Fig. 6C did not accurately represent the experimental results. Different lanes were erroneously duplicated. *Lane 3* of the PATZ panel was duplicated in *lane 7*; *lane 4* of the PATZ panel was duplicated in *lanes 5 and 6*; *lane 1* of the BCL6 panel was duplicated in *lane 2*; *lane 4* of the tubulin panel was duplicated in *lane 7*; and *lane 5* of the tubulin panel was duplicated in *lane 6*. The authors have provided an image from a replicate experiment. This correction does not affect the interpretation or conclusions of this work.



| | Patz1+/+ | | | Patz1+/− | | | |
|---|---|---|---|---|---|---|---|
| | N | | | Hy | | Ly | |
| PATZ/tub | 1 | 1.1 | 0.44 | 0.57 | 0.43 | 0.76 | 0.50 |

Raffaela Pero, Dario Palmieri, Tiziana
Angrisano, Teresa Valentino, Antonella
Federico, Renato Franco, Francesca Lembo,
Andres J. Klein-Szanto, Luigi Del Vecchio,
Donatella Montanaro, Simona Keller, Claudio
Arra, Vasiliki Papadopoulou, Simon D.
Wagner, Carlo M. Croce, Alfredo Fusco,
Lorenzo Chiariotti and Monica Fedele